

Department of Structural Engineering
School of Civil and Environmental Engineering
Cornell University
Ithaca, NY 14853

WIND-TUNNEL STUDY OF WIND LOADING ON
OFFSHORE OIL PLATFORMS

by

Thomas A. Morreale
Peter Gergely
and
Mircea Grigoriu

December 1983

Report No. 83-7

Report to the
National Bureau of Standards, U. S. Department of Commerce

FINAL REPORT

December 15, 1983

ABSTRACT

Two models, with scales of 1/250 and 1/500, of an offshore oil platform were tested in a wind tunnel to obtain static forces for various wind directions. Two peak wind velocities were used: 54 fps and 108 fps. The measured shears and moments along wind were generally in reasonably good agreement with previous results obtained in a different wind tunnel using larger models. The agreement for transverse forces and moments and for torsion was not as satisfactory.

INTRODUCTION

This report summarizes the results of an experimental project conducted to evaluate static wind forces (shear, overturning moment, and torsion) which act on compliant offshore structures. Figure 1 shows the models which were used for measurements in a wind tunnel located in the Department of Mechanical and Aerospace Engineering at Cornell University. They represent scaled versions of the prototype shown in Fig. 2.

The study was needed because:

- i) The common analytical methods, using projected areas and drag coefficients on single elements of a structure, are usually inaccurate when applied to large structures with irregular shapes, such as offshore drilling platforms;
- ii) It has been previously shown (Refs. 1 and 5) that wind tunnel studies can provide useful information regarding wind loads if similarity criteria are satisfied (primarily geometric similarity of model dimensions and wind profile, and, in some cases, Reynolds number);
- iii) Reported measurements of wind effects on this type of offshore structure (Ref. 3) are limited to a single scale, and were obtained at a different wind tunnel facility. Therefore, a major objective of this project was to:
 - a) provide additional experimental verification of these previously published results; and
 - b) to determine the sensitivity of the measurements to scale effects at moderate and high wind speeds, and to the type of wind tunnel facility being used. This information is necessary for structural reliability studies.

CORNELL WIND TUNNEL

Figure 3 shows the Cornell Environmental Boundary-layer Wind Tunnel (Ref. 4). The major sections of the tunnel are the mouth, the fetch, the test section, the diffuser, and the fan/exhaust vane matrix.

The 32 ft. long fetch section is needed to develop a turbulent flow boundary layer. It has a height-adjustable ceiling to minimize the effect of blockage. The tests were run with cross-section dimensions of 3 ft. high by 4 ft. wide giving an area at the test section entrance of 12 ft.². Since the 10 ft. long test section is of the "open-jet" type (Fig. 3d), it permits direct access from one side to the model during operation. The diffuser inlet is designed to minimize this pressure difference and to provide a smooth transition of flow between the test section and fans.

The fans are arranged in a 3 wide-2 high matrix (Fig. 3b). They are the Buffalo Force Type "S" Adustax, Arrangement 4, Vane Axial Fans and are powered by a 2-speed (1750 and 3500 RPM), single winding, variable torque motor. The fans are equipped with variable exhaust vanes which allow additional control of the airflow and thus of the wind speed in the tunnel. They are located so that the air is drawn rather than pushed through the tunnel. The maximum speed with all 6 fans running at 1750 RPM and Vanes full-open, is $54 \frac{\text{ft}}{\text{s}}$ (37.5 mph). By switching to high-speed (3500 RPM), the maximum wind speed is approximately $108 \frac{\text{ft}}{\text{s}}$ (75 mph). These two speeds are denoted by LO and HI speeds.

Wind Profile

For engineering applications, the variation of mean wind speed with height is commonly represented by a power law profile

$$\bar{V}(z) = \bar{V}(z_R) \left[\frac{z}{z_R} \right]^\alpha$$

where z_R = some reference height above the still water level and is usually taken as 10 meters (32.8 ft.), $\bar{V}(z_R)$ = the mean speed at that height, and α = an exponent which reflects roughness conditions. According to modeling theory, geometric similarity requires that the exponent α used for wind tunnel studies be the same as the one at the site under consideration (e.g., 0.1128 for the Gulf of Mexico (3)), and the height in the tunnel be reduced according to the model scale. Figure 4a shows normalized wind profiles in the Cornell wind tunnel for both models for low speed.

To develop the necessary boundary layer and achieve the proper velocity profile, wind spires were placed upstream from the test section (See Fig. 4b). The base/height ratio of each individual spire, spacing, and distance upstream determined the exponent value. The dimensions of the spires and their locations depend on the scale of the model and were determined using formulas in Ref. 2. Additional floor roughness was achieved by using a wire mesh attached to the floor (See Fig. 3c or 5e) between the model and the spires to simulate a calm sea (5-10' swells) and to aid in refining the lower portion of the velocity profile near the floor.

The in-tunnel wind speeds were measured at various heights using a "hot-wire" anemometer. Series of measurements were taken across the test area cross section (transverse to the flow). The measurements were made at the centerline of the model location and at 6" to the left and right of the centerline. The meter was checked and calibrated using a pitot/bourdon tube device. The measurements are summarized in Table 1 for the small (SM) and large (LG) models and LO speed. The table gives exponents α and the geometrical characteristics of spires. It also shows that there are differences between the wind speed profiles used in the Cornell and Western Ontario

tunnels. These differences may affect the values of shear and moment coefficients but their practical importance could not be determined.

Models

The structure chosen for study was a typical example of the new generation of compliant structures which have already proven to be efficient both structurally and economically in deep-water oil fields (typically 1000'-2000' deep). Two simplified models of the Exxon/LENA offshore oil drilling/production platform were constructed at scales of 1:250 and 1:500 (hereafter called LG and SM, respectively), based on information in Ref. 3.

As Figs. 1 and 2 show, each model consists of a main deck (2-story), two track-mounted drilling derricks, a relatively long flare boom, 2 small cranes, 2 crews quarters with roof mounted helicopter decks, drilling packages, and tanks; also support columns, bracing, and well conductors, all of which extend to the average water level. The approximate full scale configuration and dimensions are shown in Fig. 2.

Since the object was to measure rigid body forces and not stresses in individual members, inertial and material similarity was not required. Dense hardwood was used for the deck, quarters, mounting platform, and steel for the support elements, drilling towers, and flareboom.

Due to the small scale of the models, some elements of the derricks, boom, and column group were slightly oversized by about 10-15% to account for a lack of smaller, more detailed members. However, the effect on the overall drag and flow field in these regions is very small compared to that in the bluff body areas (i.e., deck, quarters, helideck, etc.) which carry most of the wind loads.

Load Effect Measurement Devices (FMD and TMD)

Two devices were designed and fabricated to measure forces:

- 1) The force-measurement device (FMD) for overturning moment and shear; and
- 2) The torsion-measurement device (TMD) for torsion about the vertical centerline axis of the deck/support column group.

They are shown in Figs. 5 and 6, and their development was based on elementary structural mechanics concepts. The devices were composed of simple cantilevers and electrical strain gage balances to determine forces.

FMD. To measure overturning moments and shear forces, strain gages were placed in series (tension and compression) in a half-bridge circuit, and in orthogonal directions (along and transverse to wind) at two heights along a vertical, wooden cantilever with rectangular cross section. A wooden circular platform upon which the model rests was attached to the top of the cantilever whose lower end was fixed. The platform was calibrated with "pegholes" at 10° intervals from 0 to 180° with respect to the wind direction and the model can be rotated on it, the platform/cantilever remaining fixed. This is different from conventional devices, such as that used in Ref. 1, which rotate along with the model and measure wind effects along the model axes. It permits direct measurement of drag and moment forces in the direction of the wind and transverse to it; no vector resolution or axes transformations are necessary. However, the FMD is somewhat sensitive to errors in readings at the upper strain gages. These errors can be significant for orientations of the platform other than 0° and 180° , due to effects of torsion. As in Ref. 3, these effects are not always zero at 0° and 180° but are negligible for these wind directions. Torsion affects less the measurements at the bottom strain gages because bending takes on much larger values at these gages.

Two techniques were used to eliminate effects of torsion: (1) an averaging method which was applied to analyze the small model. The method averages

vibrations; and (ii) a device which permits the FMD to move only in the direction of the wind flow. As a result, effects of torsion were almost eliminated. The device consists of a light channel which was mounted rigidly on the FMD. The motion of the channel was guided by two pair of rollers supported with a plate which was attached to the bottom of the wind-tunnel floor. The device was necessary to control the vibrations of the large model but was not needed in the analysis of the SM. Although the device is not frictionless, it is characterized by very small friction forces.

The FMD (see Fig. 5) deflects under wind load thus producing voltages at the strain gages which are then read by a data acquisition system. With proper calibration, the voltage outputs may be converted to moments. The forces produce a linear moment diagram and the shear may then be calculated from the difference in the measured moments at the two heights (see Fig. 5c). The bending stiffness of the supporting column had to be relatively small to assure high enough strains that could be measured with confidence but not too small to avoid excessive vibrations.

The FMD is fitted with adjustable Airpot damping devices in both principal directions to provide an additional mechanism for controlling vibrations. The entire assembly is positioned below the tunnel floor such that when the model is placed on it, the model's support platform is flush with the tunnel floor (see Fig. 5d and 5e).

TMD. To measure torsional moments about the vertical axis central to the deck, the model was put on a different platform which could rotate about a simple, almost frictionless vertical pivot. The rotation was restricted (to a few degrees) by a thin, vertical steel strip element mounted radially to the platform, aligned on the axis of the wind direction, and fixed at the other end (see Fig. 6). Strain gages were mounted in series near the fixed end.

few degrees) by a thin, vertical steel strip element mounted radially to the platform, aligned on the axis of the wind direction, and fixed at the other end (see Fig. 6). Strain gages were mounted in series near the fixed end. When the model "twists" under a wind load, the element is bent and a voltage produced at the gages. As with the FMD, proper calibration allows conversion to torsional moments.

Instrumentation and Calibration

Standard, 1/4", A-7 type strain gages were used on the FMD and TMD. Pairs of gages were connected in series, one in tension and one in compression at the same elevation, in a half-bridge circuit to conventional Vishay Strain Indicator and Switch/Balance units. The output was read by a Hewlett-Packard 3200 series data acquisition voltmeter. Vibration was a significant problem because it resulted in large strain fluctuations of an approximate frequency of 2-3 Hz. The problem was overcome by reading strains at a rate of 25 readings/sec. and then averaging these data over periods of over 60 sec. In addition, dampers were used to attenuate the vibrations of the FMD.

The FMD and TMD were calibrated in the tunnel, before and after performing each test, using a simple pulley/weight system to apply a known moment to the cantilever element and then observing the voltage at each gage. Raw calibration data are available from the authors. Calibration was also applied to validate the averaging method. For this purpose, the pulley/weight system action was applied excentrically to the model oriented symmetrically about wind direction and calibration was executed. It was found that torsion has significant effects on strain gage readings and that the averaging method almost eliminates these effects.

TEST PROGRAM

The primary objective of the experimental test program was to measure the overall loads acting along and transverse to the wind direction, on two scale

DESIGNATION	SCALE	SPEED (MPH/FPS)	Re
SM/LO	1:500	38/55.7	$1.10 * 10^5$
SM/HI	1:500	75/110	$2.18 * 10^5$
LG/LO	1:250	38/55.7	$2.21 * 10^5$
Ref. 3 (comparison)	1:120	34/50	$4.13 * 10^5$
Full Scale "	1:1	34/50	$4.95 * 10^7$

Note: $Re = VL/\nu$ = Reynolds number
 ν = kinematic viscosity = $1.615 * 10^{-4}$ ft²/sec
 L = typical surface dimension (\approx 160 ft-full scale)

Typically, a test run consisted of:

- 1) setting up the FMD (or TMD) and attaching the model;
- 2) aligning model/FMD on tunnel axis;
- 3) zeroing electronics for data acquisition;
- 4) inputting data acquisition parameters - sample period, number of gages to be read, and mode (bending or torsion);
- 5) turning tunnel fans on;
- 6) running sampling program;
- 7) releasing model, physically rotating it 10°, and refastening it (measurements were taken for all orientations only with SM/LO case);
- 8) repeating steps 6 and 7 until model had gone through 180° rotation;
- 9) turning fans off;
- 10) recording any electronic zero drift--under zero wind load;
- 11) calibrating FMD (or TMD) and performing corrections.

As the model was rotated, the center of mass also shifted (varying in circular fashion); this induced a small sinusoidally varying moment into the FMD which needed to be subtracted from appropriate readings to get the true readings from the wind load. Corrections for zero drift were assumed to be

As the model was rotated, the center of mass also shifted (varying in circular fashion); this induced a small sinusoidally varying moment into the FMD which needed to be subtracted from appropriate readings to get the true readings from the wind load. Corrections for zero drift were assumed to be linear over the entire test. All corrections were made on raw voltages. Then, corrected voltages were converted to forces using a data reduction program written specifically for this application. Temperature variations were insignificant during experiments (approximately 1° F). Nevertheless, compensating strain gages were used to eliminate any effects of temperature variations on measurements.

Results

A convenient way of presenting the results such that they may be used to make design estimates, is to put the measured loads in the form of coefficients. When multiplied by appropriate area factors, the square of the reference wind speed, and the air density, they yield estimates of the full scale loads. The typical relationship for drag force and wind velocity is

$$F_D = \left[\frac{1}{2} \rho A \bar{V}^2(z_R) \right] C_D$$

where ρ is the mass density of air, A = projected area, C_D = drag coefficient, and $\bar{V}(z_R)$ = the velocity at some reference height (160 ft. full scale, in our case). The projected area for the entire structure is not easily calculated and also varies with the orientation of the structure to the wind; however, the changing projected areas are reflected in the direct measurement of forces. So a convenient way of presenting the drag coefficient for the scale model is

$$C_D = \frac{F_D}{\frac{1}{2} \rho V^2 A_R}$$

where F_D is measured and A_R is a constant reference area. The same applies to overturning moment and torsion coefficients

$$C_M = \frac{M}{\frac{1}{2} \rho V^2 A_R L_R}$$

$$C_T = \frac{T}{\frac{1}{2} \rho V^2 A_R L_R}$$

where M (or T) is measured and L_R is a reference length.

There are 5 such coefficients representing the shear (drag) force along the wind direction, the shear force transverse to the wind direction, the overturning moment along, the overturning moment transverse, and torsion about the center z axis. They are denoted, respectively, C_{DA} , C_{DT} , C_{MA} , C_{MT} , C_T , and have a (+) sign convention as shown in Fig. 7.

The total shear (drag) is constant over the height of the structure; however, the overturning moments are referenced to a point 553' below the water level. This point is neither significant nor is it arbitrary; it simply arises from the geometry of the FMD (see Fig. 5c). In making a full scale estimate one need only know the moment and shear at one point to determine the moment at any other point of interest (e.g., at the foundation/structure interface) since the gross moment diagram due to wind load is linear. Also, it is not necessary to know the actual projected area of the structure; only the scale ratio. Thus, if the coefficients were obtained for 1:500 scale

model using $A_R = 1 \text{ ft.}^2$ and $L_R = 1 \text{ ft.}$, the full scale load for $z = -553 \text{ ft.}$ would be:

$$F_D = \left[\frac{500}{1} \cdot 1 \right]^2 \frac{1}{2} \rho \bar{V}^2 C_D$$

$$M = \left[\frac{500}{1} \cdot 1 \right]^2 \left[\frac{500}{1} \cdot 1 \right] \frac{1}{2} \rho \bar{V}^2 C_M$$

Typical values are:

$$M = 377,000 C_M \text{ (in k-ft.)}$$

$$\text{for } \rho = .002231 \frac{\text{lb} \cdot \text{sec}^2}{\text{ft}^4} \text{ \& } \bar{V}_R^2 = 52 \frac{\text{ft}}{\text{s}}$$

The coefficients obtained from this project are shown in Fig. 8 and Tables 2-6 as a function of structural orientation. In order to compare them with those obtained in Ref. 3, which is based on $A_R = 1 \text{ ft.}^2$, $L_R = 1 \text{ ft.}$, and a scale of 1:120, the following reference areas/lengths were used:

$$A_R = \left[\frac{120}{250} \cdot 1 \right]^2 \text{ \& } \left[\frac{120}{500} \cdot 1 \right]^2 = .23 \text{ \& } .06$$

$$L_R = \left[\frac{120}{250} \cdot 1 \right] \text{ \& } \left[\frac{120}{500} \cdot 1 \right] = .48 \text{ \& } .24$$

for the 1:250 and 1:500 models, respectively. Furthermore, the moment coefficients for the small and the large models and those in Ref. 3 were reduced to the same depth $z = -553 \text{ ft.}$, based on a moment-shear relationship. To determine full scale estimates of design wind loads one should multiply the

coefficients in Fig. 8 or Tables 2-6 by $\frac{1}{2} \rho \bar{V}^2 A_R$ for drag and $\frac{1}{2} \rho \bar{V}^2 A_R L_R$ for moment, in which $A_R = (120)^2$ ft. and $L_R = 120$ ft. These reference values for area and length correspond to the scale of the model in Ref. 3 taken as reference in this study.

Figure 8 and Tables 2-6 show the variation of the coefficients C_{DA} , C_{DT} , C_{MA} , C_{MT} , and C_T with wind direction. Results are based on experiments performed at Cornell University and Western Ontario University (as reported in Ref. 3). The tables also give percentage differences between Cornell and Western Ontario findings. They are generally in the range 10-30% for along wind shear and bending moments acting on the SM but are smaller for the LM (generally less than 15%). The differences become larger for transverse wind effects. However, these differences are not critical for design because across wind effects are very small, approximately 5% of the along wind effects. From Fig. 8(c) and Table 6, torsion coefficients vary significantly with wind speed, model scale, and wind tunnel type.

Differences of such magnitudes as those found in this study are not uncommon in wind tunnel studies, see Ref. 6 for comparisons between pressure measurements on models varying in scale from 1/100 to 1/500. The magnitude of these differences depends on:

(i) model scale, 1:120 in Ref. 3 versus 1:500 (SM) and 1:250 (LG) in Cornell experiments. Effects of model scale can be evaluated, e.g., from Tables 2 and 5. They can be as high as 30% for some orientations. Note that these affects can be affected slightly by differences between wind speed profiles;

(ii) wind speeds, 50 fps in Ref. 3 versus 54 fps (LO) and 108 fps (HI) in Cornell experiments;

(iii) wind tunnel type. As previously mentioned, the Cornell tunnel is of open-jet type, as it has an open test section (Fig. 3a), while the test section is closed at the University of Western Ontario wind tunnel; and

(iv) inherent experimental errors. For example, errors in the determination of the wind speed of 5% can account for 10% variations in the drag and moment coefficients. From wind speed data in Table 1, such errors are not unlikely to occur. The uncertainty in calibration factors can also influence adversely measurements, particularly the location of the center of wind pressures. For example, 2% and -2% errors in the calibration factors of the top and bottom strain gages result in drastic changes of the wind pressure center, from 95 ft above the still water level at $\theta = 90^\circ$ to 140 ft (+47% error). On the other hand, the errors in bending moment and shear are respectively -2% and -8%. Similar results can be found for all other directions. It can be concluded that the FMD provides very accurate measurements for bending moments and satisfactory readings for shear forces. However, the location of the center of wind pressures is less accurate. For the SM/L0 case, it varies from 80 ft to 216 ft. The elevation of the center of wind pressures increases steadily with θ for orientations $\theta > 90^\circ$ due to effects of uplift forces.

CONCLUSIONS

Two models, with scales of 1/250 and 1/500, of an offshore drilling platform were tested in a wind tunnel to obtain static forces for various angles of the wind velocity. Two wind velocities were used: 54 fps and 108 fps (37.5 mph and 75 mph). The measured shears, moments, and twists were found to be in reasonably good agreement with previous results obtained in a different wind tunnel using larger models.

It was found that:

i) along wind drag and moment coefficients determined from experiments performed in the Cornell and the Western Ontario wind tunnels depend similarly on wind direction. However, the magnitude of these coefficients differ generally by 10 to 30% for the SM and less than approximately 15% for the LG;

ii) differences were noted between transverse and torsional coefficients obtained from the Cornell and the University of Western Ontario wind tunnels. These differences were not fully understood. Errors in measurements may have significant contributions because these effects have generally small values. The magnitude of these errors is difficult to assess;

iii) the variation of the drag coefficients with model scale and wind speed (Tables 2 and 4) suggests that these coefficients depend to some extent on the Reynolds number over the range of values considered in Ref. 3 and in this study; and

iv) the differences between wind effect coefficients obtained from experimental studies in the Cornell and Western Ontario wind tunnels suggest that there is a sizable uncertainty in these coefficients. This uncertainty should be incorporated in design to assure a realistic representation of wind effect.

REFERENCES

1. Cermak, J. E., "Wind-Tunnel Testing of Structures," Journal of the Engineering Mechanics Division, ASCE, Vol. 103, No. EM6, Proc. Paper 13445, December, 1977, pp. 1125-1140.
2. Irwin, H. P. A. H., "The Design of Spires for Wind Simulation," Journal of Wind Engineering and Industrial Aerodynamics, Vol. 7, 1981, pp. 361-366.
3. Pike, P. J., and Vickery, B. J., "A Wind-Tunnel Investigation of Loads and Pressures on a Typical Guyed Tower Offshore Platform," presented at the May 3-6, 1982, 14th Annual Offshore Technology Conference, held at Houston, Texas.
4. Ribando, R. J., "The Cornell Environmental Wind Tunnel," M.S. Thesis, The Sibley School of Mechanical and Aerospace Engineering, Cornell University, Ithaca, NY, August, 1974.

5. Simiu, E., and Scanlan, R. H., Wind Effects on Structures, John Wiley and Sons, 1978.
6. Simiu, E., "Modern Developments in Wind Engineering", Engineering Structures, October, 1981, pp. 242-248.

TABLES AND FIGURES CAPTIONS

Table 1 - Wind Profile Data

Table 2 - SM/LO Along Wind

Table 3 - SM/LO Across Wind

Table 4 - SM/HI Along Wind

Table 5 - LM/LO Along Wind

Table 6 - Torsion Coefficients

Fig. 1 - Models of an Offshore Structure

Fig. 2 - Offshore Structure Prototype

Fig. 3 - Cornell Wind Tunnel

Fig. 4 - Wind Profile

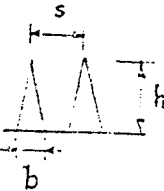
Fig. 5 - Force-Measurement Device

Fig. 6 - Torsion-Measurement Device

Fig. 7 - Sign Convention

Fig. 8 - Wind Effect Coefficients

*** Table 1.- Wind Speeds (in meters/sec) ***

Size/Speed	SM/LO			LG/LO		
HT (INS)	LEFT	CENTER	RIGHT	LEFT	CENTER	RIGHT
0+	7.9	7.7	7.8	8.7	8.5	8.6
1.5	12.3	12.1	12.2	13.0	13.0	12.9
2	12.8	12.7	12.6	13.6	13.7	13.7
3	13.7	13.7	13.5	13.9	13.9	13.9
4	14.9	14.9	15.0	14.9	14.9	15.0
5	15.7	15.6	15.6	15.1	15.2	15.3
6	16.2	16.2	16.1	15.3	15.3	15.5
7	16.5	16.5	16.5	15.8	15.8	15.7
8	16.7	16.7	16.6	16.2	16.1	16.0
9	16.8	16.8	16.7	16.3	16.3	16.1
10				16.6	16.6	16.4
	$\alpha = 0.152$			$\alpha = 0.130$		
	$b = 1.0''$			$b = 2.0''$		
	$h = 10.5''$			$h = 21.0''$		
	$s = 4.5''$			$s = 9.0''$		

1 m/sec = 3.28 fps

Table 2. -- SM/LO Along Wind

Orientation θ	Cornell Tests		Ref. 3		Differences (%)	
	C_M	C_D	C_M	C_D	C_M	C_D
0	10.70	1.99	8.21	1.50	30	33
10	11.18	2.12	8.41	1.52	33	39
20	11.69	2.14	9.25	1.68	26	27
30	12.19	2.14	9.98	1.81	22	18
40	12.70	2.29	10.43	1.89	22	21
50	12.67	2.23	10.36	1.88	22	19
60	12.14	2.16	9.85	1.78	23	21
70	11.51	2.06	8.96	1.61	28	28
80	10.03	1.90	8.13	1.47	23	29
90	9.52	1.76	7.81	1.42	22	24
100	10.27	1.89	8.28	1.49	24	27
110	11.46	2.06	9.28	1.66	23	24
120	12.11	2.01	10.28	1.83	18	10
130	12.80	2.12	10.92	1.92	17	10
140	12.86	2.04	11.77	2.08	9	-0.02
150	12.86	2.09	11.46	2.00	12	5
160	12.04	1.88	10.45	1.80	15	4
170	11.25	1.85	10.14	1.73	11	7
180	11.31	1.86	10.23	1.75	11	6

Table 3. -- SM/LO Across Wind

Orientation θ	Cornell Tests		Ref. 3		Differences (%)	
	C_M	C_D	C_M	C_D	C_M	C_D
0	-0.03	-0.15	-0.16	-0.04	19	375
20	0.83	0.02	-0.53	-0.08	157	400
40	0.44	0.19	-0.51	-0.08	14	238
60	0.38	0.01	-0.24	-0.04	58	400
90	0.20	0.05	0.11	0.04	82	25
120	0.30	0.11	0.87	0.14	66	21
160	1.68	0.20	1.43	0.24	17	20
180	1.80	0.12	0.00	0.00	---	---

Table 4. -- SM/HI Along Wind

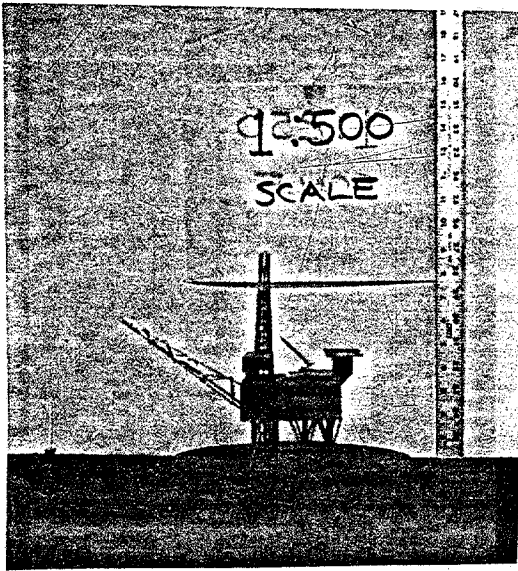
Orientation θ	Cornell Tests		Ref. 3		Differences (%)	
	C_M	C_D	C_M	C_D	C_M	C_D
0	9.73	1.95	8.21	1.50	19	30
180	10.61	2.27	10.23	1.75	4	30

Table 5. -- LG/LO Along Wind

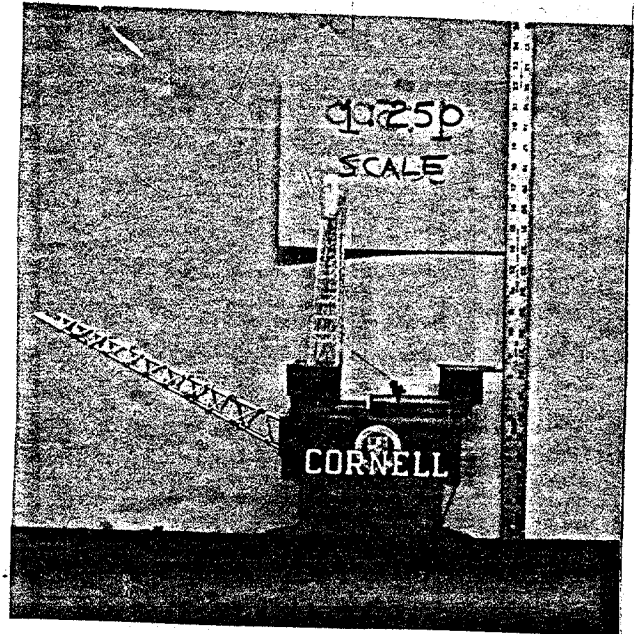
Orientation θ	Cornell Tests		Ref. 3		Differences (%)	
	C_M	C_D	C_M	C_D	C_M	C_D
0	8.08	1.52	8.21	1.50	2	1
20	9.40	1.76	9.25	1.68	2	1
40	10.23	1.88	10.43	1.89	2	5
60	10.31	1.94	9.85	1.78	5	1
90	8.41	1.62	7.81	1.42	8	14
120	11.61	2.08	10.28	1.83	13	14
160	12.02	2.20	10.45	1.80	15	22
180	11.42	2.08	10.23	1.75	12	19

Table 6. -- Torsion Coefficients

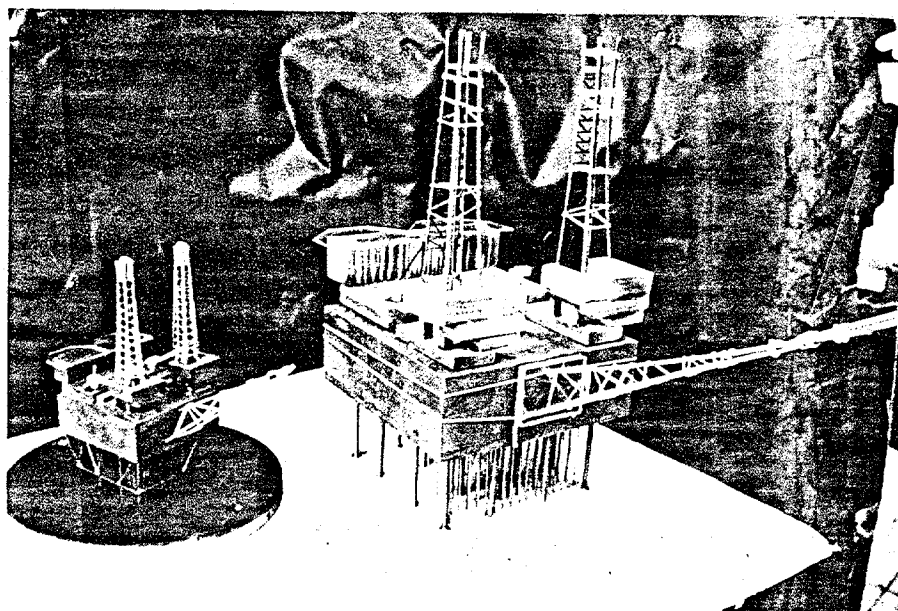
Orientation θ	Cornell Tests			Ref. 3
	SM/LO	SM/HI	LG/LO	
0	0.00	0.08	0.08	-0.02
10	0.01	0.08	0.08	-0.05
20	0.06	0.15	0.18	-0.03
30	0.13	0.31	0.39	0.02
40	0.22	0.47	0.53	0.08
50	0.30	0.53	0.65	0.14
60	0.37	0.60	0.68	0.21
70	0.38	0.60	0.67	0.23
80	0.34	0.54	0.56	0.19
90	0.28	0.47	0.49	0.17
100	0.29	0.50	0.48	0.17
110	0.29	0.49	0.53	0.18
120	0.27	0.53	0.57	0.22
130	0.24	0.50	0.55	0.25
140	0.19	0.43	0.51	0.28
150	0.16	0.38	0.48	0.30
160	0.10	0.28	0.38	0.28
170	0.04	0.14	0.20	0.16
180	-0.06	-0.06	0.04	0.00



(a) Small (SM)



(b) Large (LG)



(c) Both (large model is not completed)

Fig. 1 Photos of Models

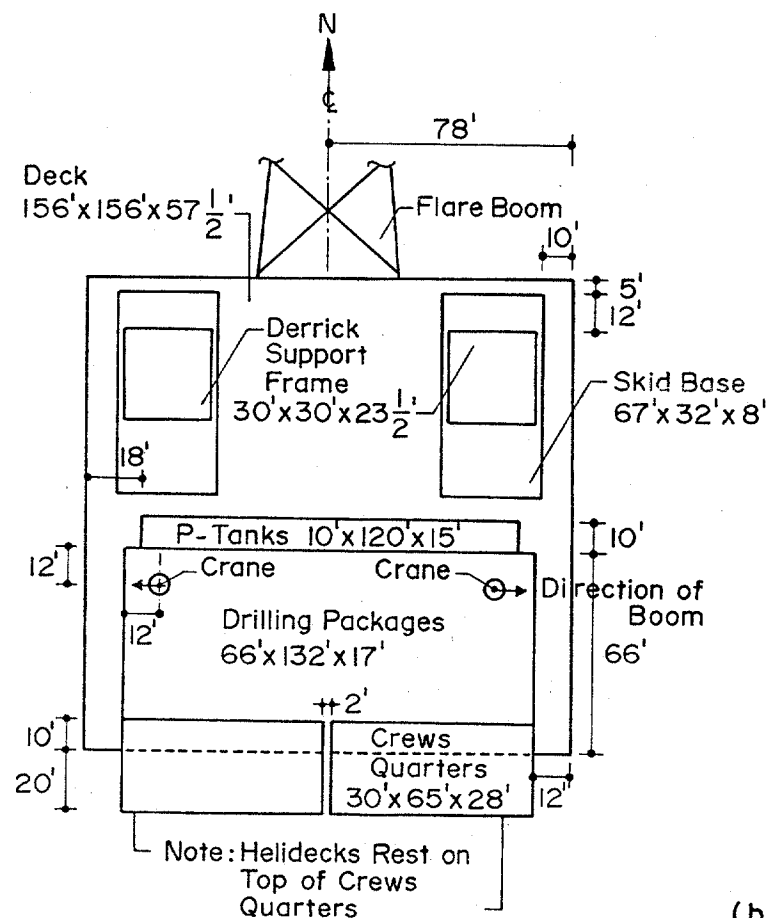
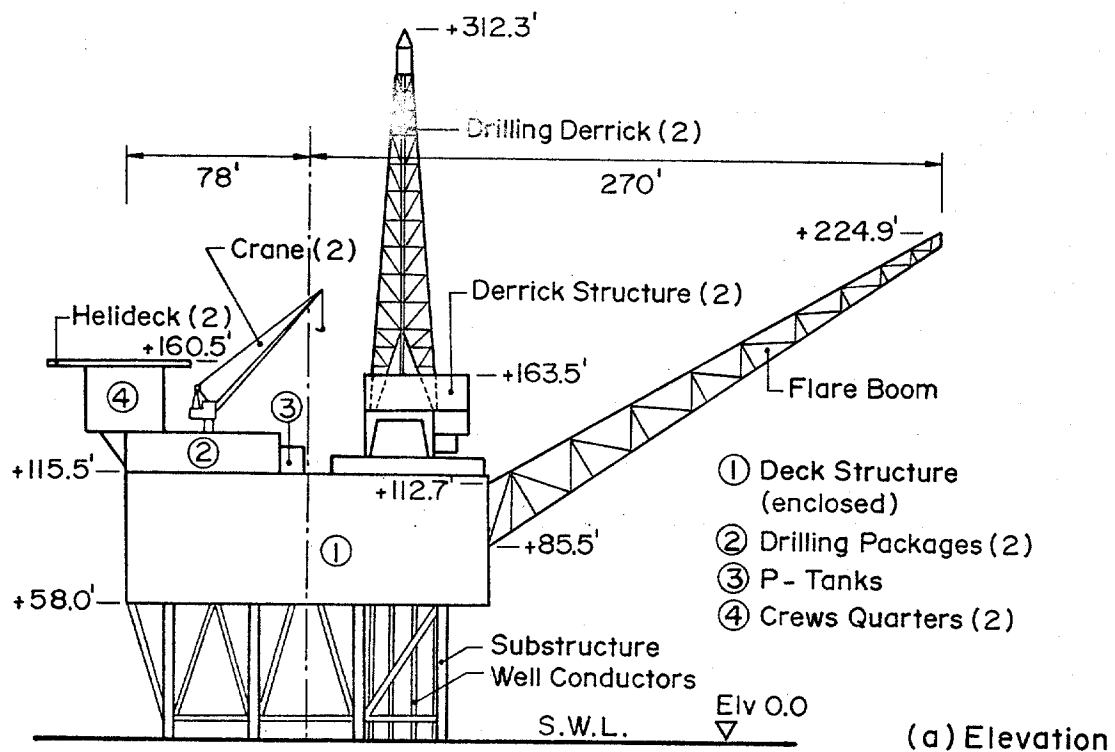
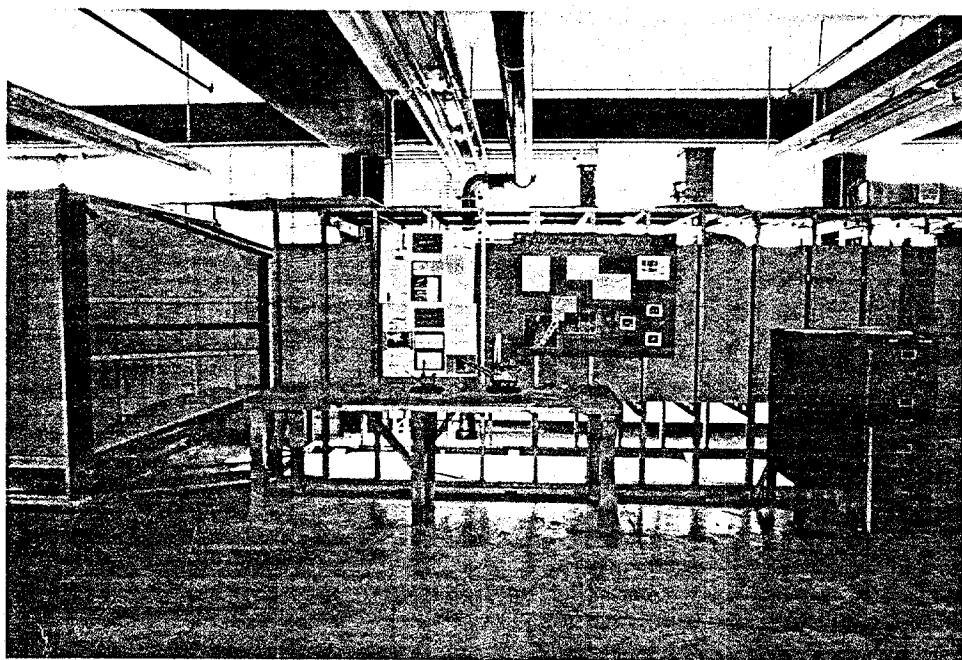
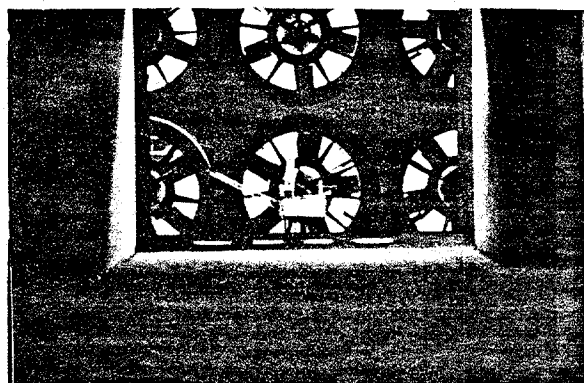


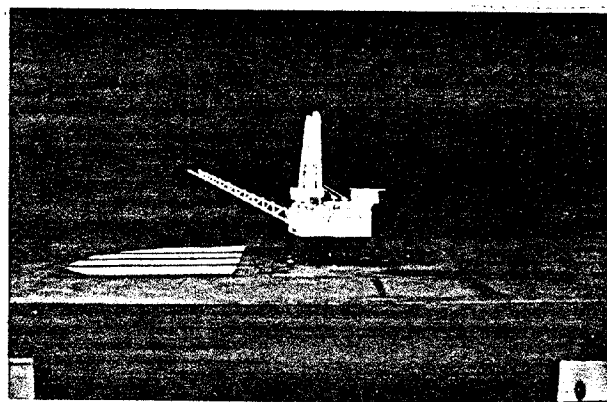
Fig. 2 Drawings of Prototype Structure



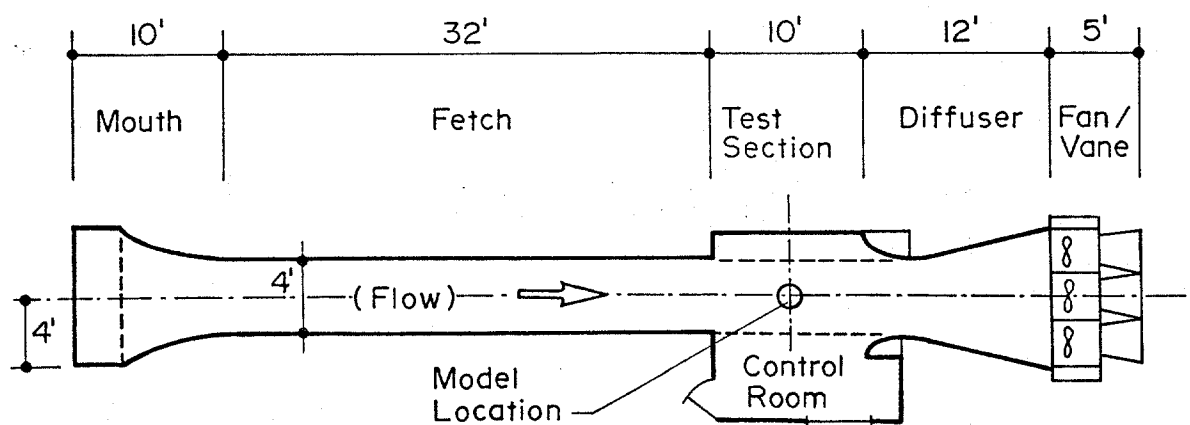
(a)



(b)



(c)



(d)

Fig. 3 Cornell Boundary Layer Tunnel

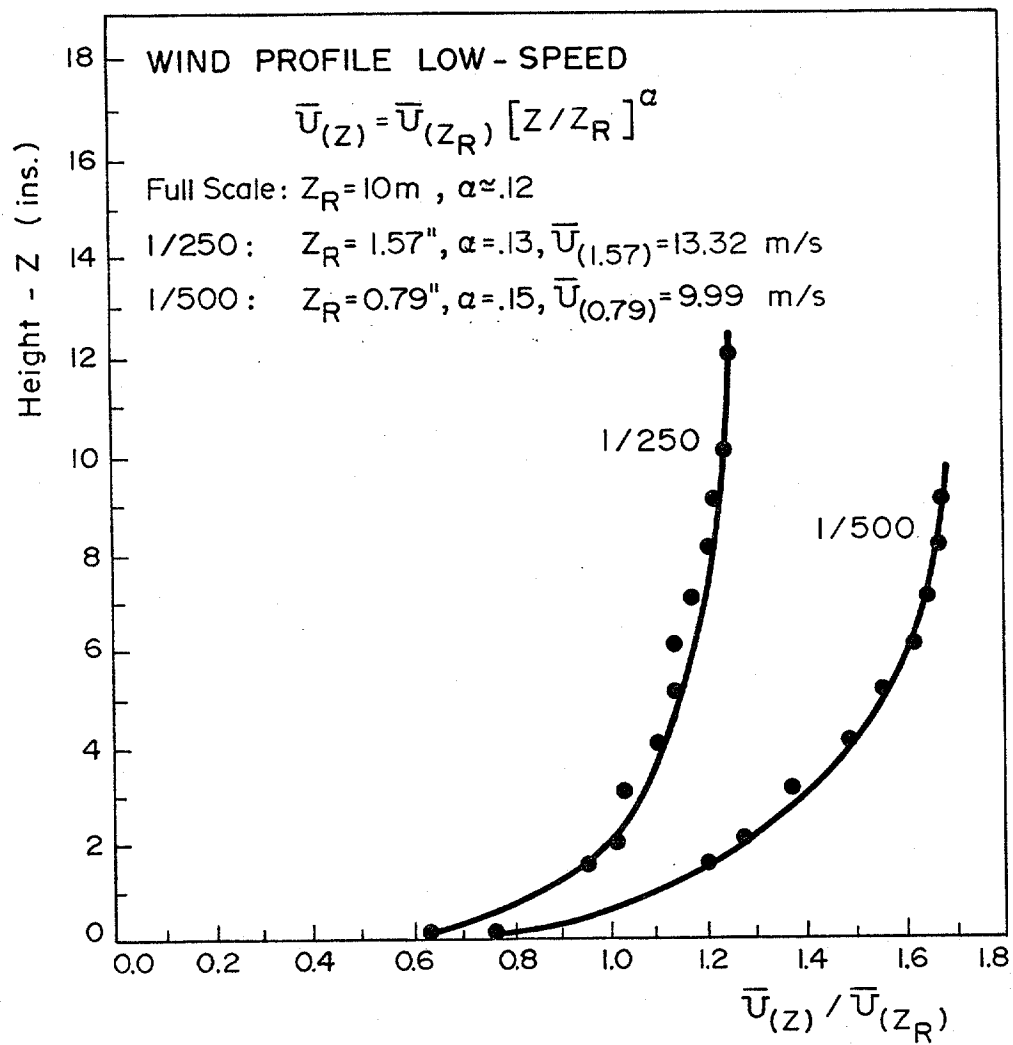


Fig. 4a Wind Profile (Low Speed)

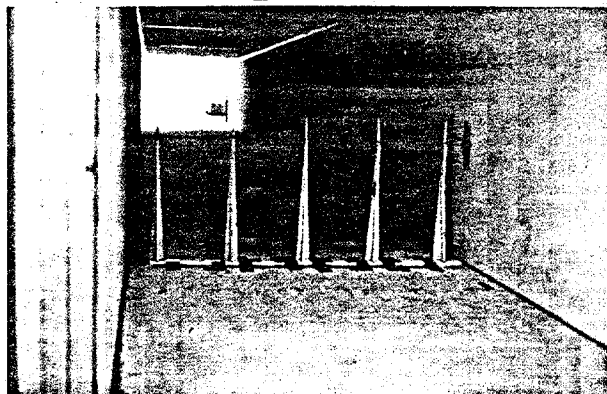
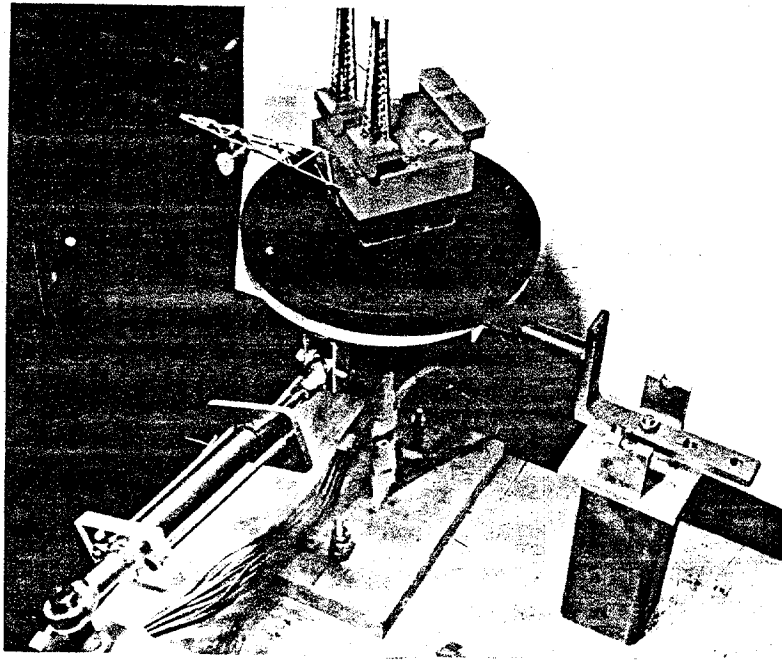
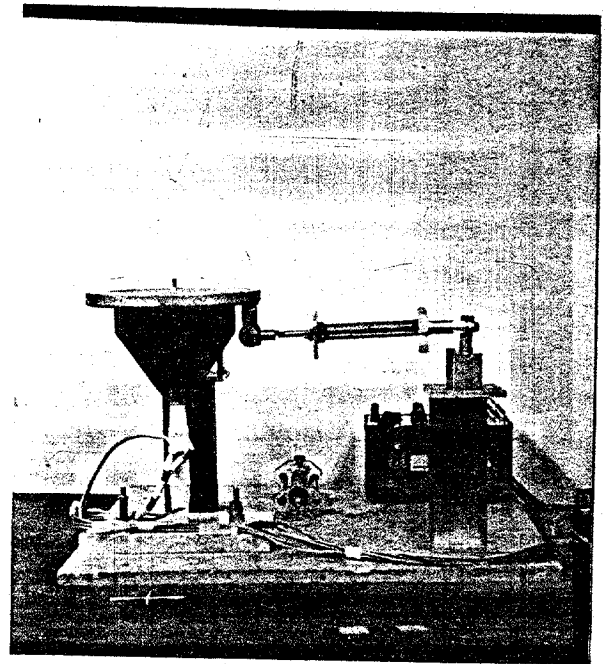


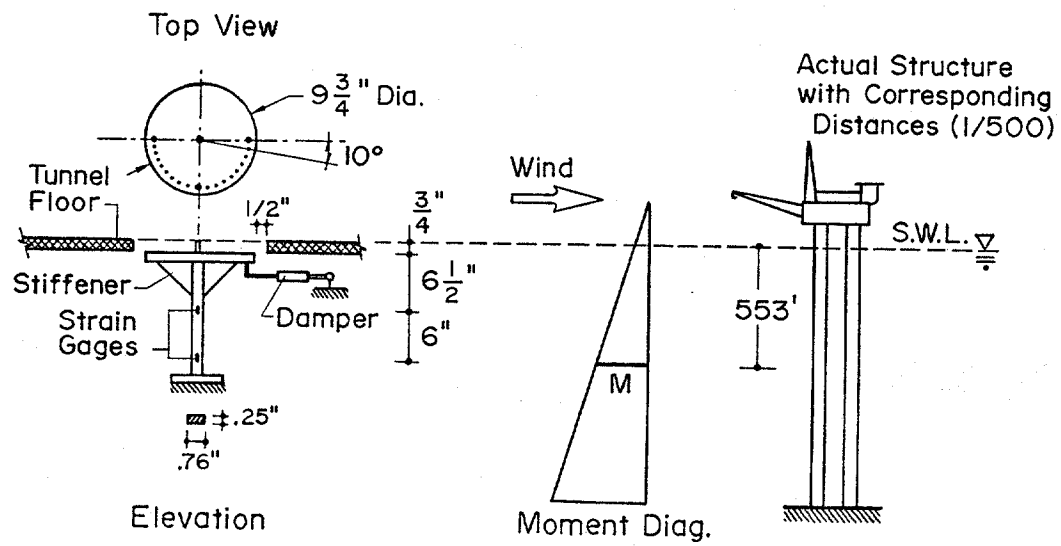
Fig. 4b Wind Spires (LG)



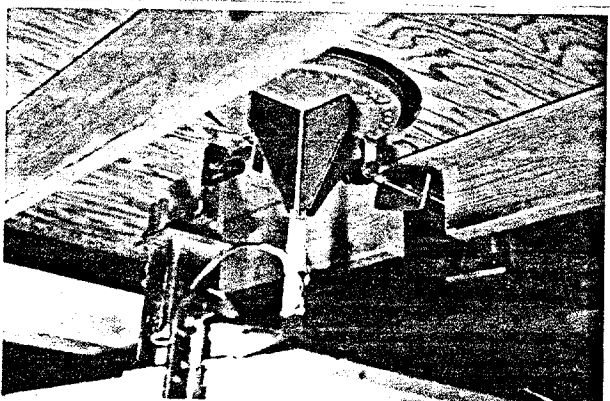
(a)



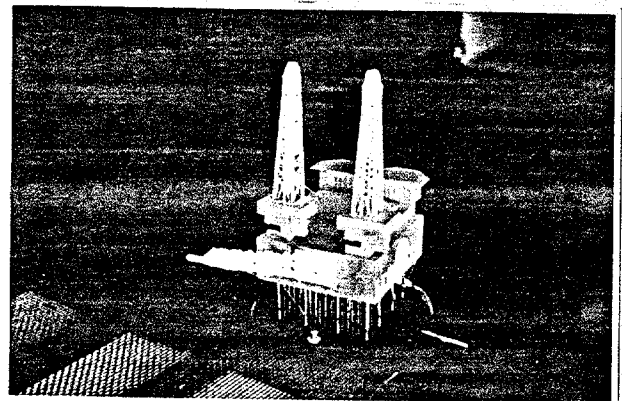
(b)



(c)

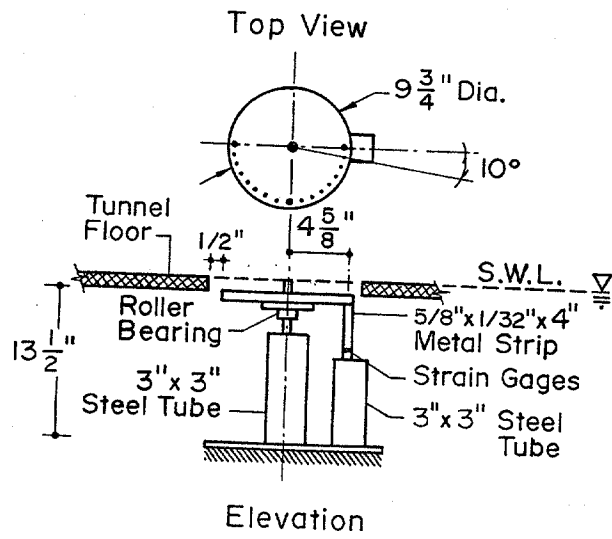


(d)

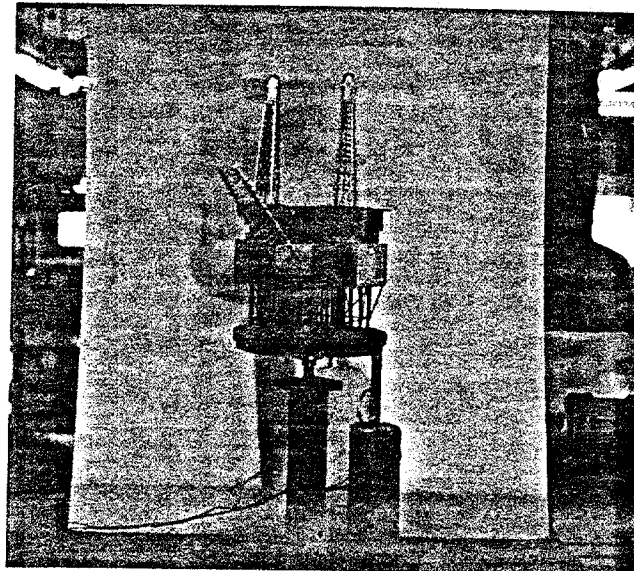


(e)

Fig. 5 Force Measurement Device



(a)



(b)

Fig. 6 Torsion Measurement Device

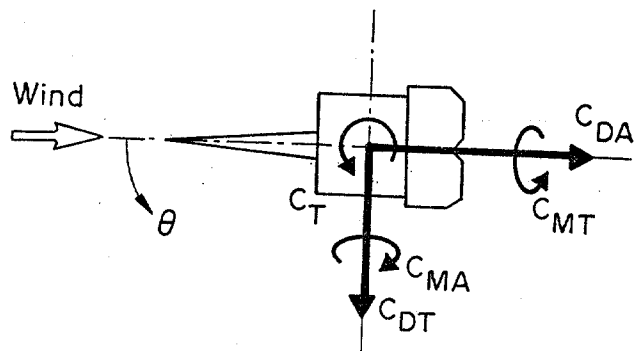


Fig. 7 Sign Convection

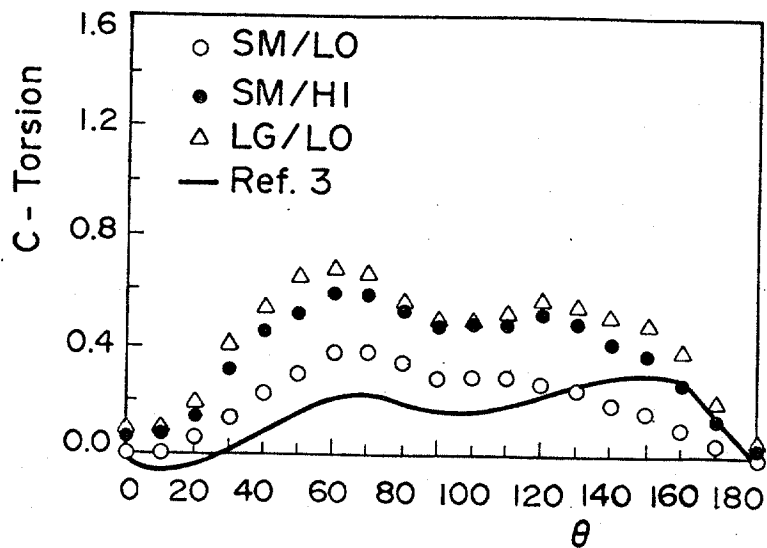
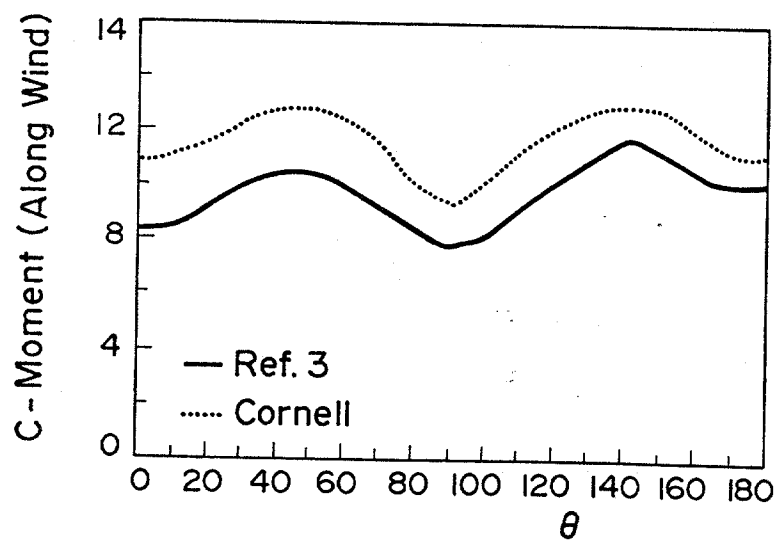
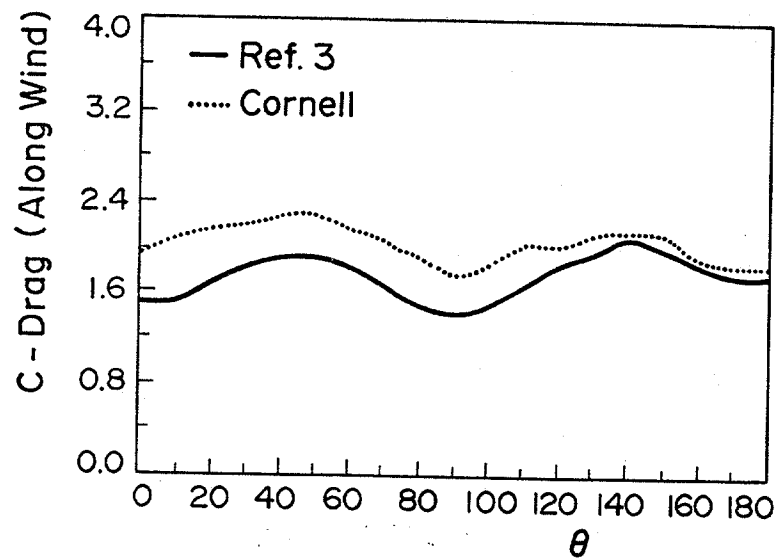


Fig. 8 Wind Effect Coefficients